Dynamic analysis of widely tunable laser diodes integrated with sampled- and chirped-grating distributed Bragg reflectors and an electroabsorption modulator

Byoung-Sung Kim, Youngchul Chung, and Sun-Ho Kim*

Dept. of Electronic Communications Eng., School of Electronics Eng.
Kwangwoon University, 447-1 Wolgye-Dong Nowon-Ku, Seoul, Korea 139-701

**Division of Information and Electronics Korea Institute of Science and Technology, Seoul, Korea 136-791*

Abstract

Widely tunable laser diodes integrated with periodically sampled and chirped DBR(distributed Bragg reflector) and an EA(electroabsorption) modulator are analyzed dynamically using the improved large-signal time-domain model. The tuning characteristics of sampled- and chirped-grating DBR laser diodes are demonstrated theoretically. The results of the simulation agree well with those of the experiment. And the intensity-modulation properties of the laser diodes integrated with an EA modulator are calculated. It is shown that the external modulation has the lower frequency chirp by 1/20 for the same extinction ratio than the direct modulation, and also the short pulse train can be generated using the optical gating of an EA modulator.

Keywords: Integrated optics, Semiconductor lasers, Electroabsorption modulator

1. Introduction

Wavelength tunable laser diodes are critical components in a wide variety of WDM(wavelength division multiplexing) and packet switching architectures[1,2]. And also wavelength-tuned short pulses generated from the semiconductor laser diodes are of great importance for the developments of ultrahigh speed and WDM optical communication systems[3].

Over the past several years, both continuously and discontinuously tunable lasers incorporating periodically sampled and chirped grating have been studied theoretically and experimentally[4-10]. The laser diodes with wide tunability have several active and/or passive sections, and include Bragg gratings. These laser diodes show the wide tuning range of above 60 nm, stable lasing condition, and large side-mode suppression ratio.

Directly modulated semiconductor laser diodes, even those with a single mode, exhibit a dynamic frequency chirp that is induced by changes in the carrier density as the laser turns on and off. The dynamic linewidth broadening caused by such a large frequency chirp can result in a significant penalty in the performance of high-speed long-haul optical communication systems. The CW (continuous wave) laser diodes integrated with an

external EA modulator are an breakthrough to realize the high-speed optical systems with low chirp.

And the short pulse generation using the external modulator has been realized experimentally, whose principle of the pulse generation is the optical gating of the electroabsorption modulator which is driven by the sinusoidal signal[11,12]. The short optical pulses have many applications ranging from optical communications systems, optical switching, electro-optic sampling, optical sampling systems to optical analog-to-digital conversion[13-18].

In this paper, widely tunable laser diodes incorporating periodically sampled and chirped gratings and an external modulator are analyzed using an improved time-domain dynamic model. First, it is demonstrated that the improved model is very powerful in simulating the complex laser diodes with active and passive sections. And, the dynamic properties of the sampled grating DBR and chirped grating DBR laser diodes are investigated. Second, the modulation characteristics of the laser diode integrated with the external electroabsorption modulator are studied. It is shown that the external modulation are superior to the direct modulation in the aspect of the lower frequency chirp. And the pulse generation by the optical gating of the external modulator is observed theoretically.

The paper is organized as follows. A description of the improved time-domain dynamic model is presented in Section 2. Section 3 discusses the tuning characteristics of the widely tunable laser diodes integrated with sampled- and chirped-grating distributed Bragg reflectors. Section 4 describes the intensity-modulation properties of the laser diode incorporating the external electroabsorption modulator. Finally, Section 5 gives a brief conclusion.

2. The improved large-signal time-domain model

The time-domain model used for the evaluation of the widely tunable laser diodes integrated with sampled- and chirped-grating DBR and a EA modulator is based on the model described in the reference[19]. The electrical field in the waveguide can be written as

$$E(z,t) = [F(z,t)e^{-i\beta_0 z} + R(z,t)e^{i\beta_0 z}]e^{i\omega_0 z} \quad (1)$$

where ω_0 is the reference frequency and β_0 is the propagation constant at Bragg frequency. F(z,t) and R(z,t) represent the forward and reverse waves propagating along the longitudinal direction, z in this paper, respectively. The fields F(z,t) and R(z,t) satisfy the time-dependent coupled wave equations

$$\frac{1}{v_g}\frac{\partial F(z,t)}{\partial t} + \frac{\partial F(z,t)}{\partial z} = (g - \alpha - i\delta)F(z,t) + i\kappa R(z,t) + S_f \quad (2a)$$

$$\frac{1}{v_g}\frac{\partial R(z,t)}{\partial t} - \frac{\partial R(z,t)}{\partial z} = (g - \alpha - i\delta)R(z,t) + i\kappa F(z,t) + S_r. \quad (2b)$$

Here, the complex fields F and R contain the amplitude and phase information. V_g is the group velocity, which is assumed to be constant over the frequencies of interest, κ is the coupling coefficient between the forward and reverse waves, α is the summation of the waveguide loss and the electroabsorption loss. The spontaneous noise coupled into the forward and reverse fields are given as S_f and S_r, respectively. The spontaneous emission fields coupled to the forward and reverse waves have equal amplitudes, $S_f(z,t) = S_r(z,t) = S(z,t)$[20]. The emission is then assumed to have a Gaussian distribution and to satisfy the correlation

$$\langle S(z,t)S^*(z',t')\rangle = \beta R_{sp}\delta(z-z')\delta(t-t')/v_g \quad (3a)$$

$$\langle S(z,t)S(z',t')\rangle = 0. \quad (3b)$$

where R_{sp} equals BN^2/L and is the electron-hole recombination rate per unit length contributed to the spontaneous emission. In the above B is the spontaneous recombination coefficient, L is the length of the active region, N is the carrier density, β is the spontaneous coupling factor, and $\delta(x)$ is defined as the δ-function.

In the active region, the field gain is given by

$$g(z,t) = \frac{\Gamma g_N \{N(z,t) - N_0\}}{2(1+\varepsilon P)} \quad (4)$$

where Γ is the confinement factor of the active layer, g_N is the differential gain, N_0 is the carrier density at transparency, ε is the gain compression coefficient, P is the photon density, and δ is the detuning factor which means the deviation from Bragg conditions and given by

$$\delta = \frac{\omega_0}{c}(n_{eff,0} + \Delta n) - \frac{\pi}{\Lambda} \quad (5a)$$

$$\Delta n = -\frac{\lambda_0}{4\pi}\Gamma \alpha_m g_N \Delta N(z,t) \quad \text{in the active region} \quad (5b)$$

Here, c is the speed of light in vacuum and Λ is the pitch of the grating. $n_{eff,0}$ is the effective refractive index without injection current, that is, when the carrier density $N = N_0$, ΔN is the change of carrier density, and α_m is the material linewidth enhancement factor.

The time-dependent carrier rate equation in the active region is given by

$$\frac{dN}{dt} = \frac{J}{ed} - BN^2 - CN^3 - \frac{v_g g_N (N - N_0) P}{1 + \varepsilon P} \quad (6)$$

where J is the current injection density, e is the electron charge, d is the thickness of the active layer, C is the Auger recombination coefficient, respectively, and P is the photon density given by the normalized power $\left\{|F|^2 + |R|^2\right\}$.

If we choose z = 0 at the left-hand facet, the boundary condition for the forward and reverse waves at the facets can be written as

$$F(0, t) = r_1 R(0, t), \quad (7a)$$

$$R(L_{tot}, t) = r_2 F(L_{tot}, t) \quad (7b)$$

where r_1 and r_2 are the amplitude reflectivities of the left-hand and right-hand facets, respectively, and L_{tot} is the total length of the device.

The time-dependent coupled wave equations can be numerically solved by dividing the laser into a number of small subsections with equal length of $\Delta z (= v_g \Delta t)$. And adapting the finite difference approximation to the time-dependent coupled wave equations equation and neglecting the second derivatives, the following time-stepping algorithm can be obtained:

$$F(z+\Delta z, t+\Delta t) = [(g-\alpha)\Delta z]F(z,t) + e^{-i\delta\Delta z}F(z,t) + i\kappa\Delta z R(z,t) \quad (8a)$$

$$R(z-\Delta z, t+\Delta t) = [(g-\alpha)\Delta z]R(z,t) + e^{-i\delta\Delta z}R(z,t) + i\kappa\Delta z F(z,t). \quad (8b)$$

If the field value at location z and time t is known, the forward(reverse) field at the next time $t + \Delta t$ can be determined at position $z+\Delta z$ ($z-\Delta z$) from eq. (8). This algorithm is very powerful in modeling the complex laser diodes with both the active and the passive sections. For example, the conventional algorithm[19] reveals the unstability problem when the detuning factor is very large, which is inevitable in the simulation of the widely tunable laser diode. Fortunately, $\delta\Delta z$, $\kappa\Delta z$ are usually much smaller than 1, then $(1\text{-}i\delta\Delta z)$ in the conventional algorithm can be replaced by $e^{-i\delta\Delta z}$ which should be the original phase factor over the distance Δz. Through this replacement the correct phase can be incorporated with the power conserved, even if the detuning factor δ is quite large. The effectiveness of the modification will be shown shortly.

The finite gain bandwidth in the active region can be modeled using the infinite impulse response filter[21] and is implemented as follows in the model:

$$F(z+\Delta z, t+\Delta t) = F(z,t) + A\{F(z+\Delta z, t) - F(z,t)\} \quad (9)$$

where $A = \eta \exp(j\omega_0 \Delta t)$, η and ω_0 determine the bandwidth and the center of the gain curve as a function of wavelength.

In each time step, the detuning factor δ, field gain g, and carrier density N will change according to eq. (4-6). When the forward and reverse waves reach the facets, the boundary condition must be satisfied. The spontaneous noise is generated from

a Gaussian distributed random number generator, and it satisfies the correlation in eq. (3). Since the material and structure parameters are allowed to change between different subsections, the spatial hole burning is automatically taken into account, and allows for dynamic changes in the electronic part of the refractive index, which is valuable in calculating the correct phase changes.

3. The tuning characteristics

In this section, the dynamic tuning properties of sampled-grating DBR and chirped-grating DBR laser diodes are analyzed and compared to each other. Fig. 1 shows the schematic longitudinal cross section of the device. The device is 1470 μm long, active region is 480 μm long, and rear/front reflectors are 495 μm long, respectively. The period of the rear grating modulation is 49.5 μm.

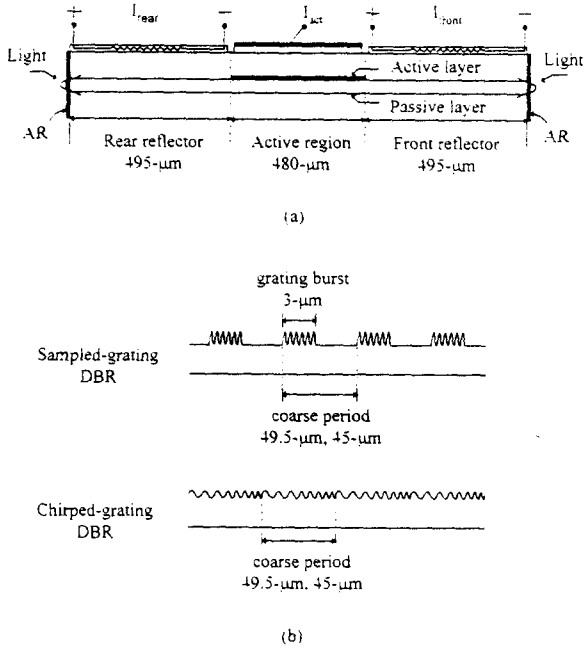

Fig. 1 Schematic drawing of (a) the longitudinal cross section of the DBR laser diodes and (b) the reflector configurations of sampled grating DBR and chirped grating DBR.

On the other hand, the period of front grating modulation is 45 μm long. In the sampled grating DBR laser diode, the length of the burst gratings is 3 μm. In the chirped grating DBR laser diode, the grating pitch varies in such a way that the Bragg wavelength increases from 1.5 μm to 1.6 μm in a coarse period when there is no index change in the grating region. The large change of the grating pitch in a coarse period results in the large bandwidth. Coupling coefficients are 200 cm^{-1}, 70 cm^{-1}, respectively for sampled- and chirped-grating DBR. When there is no index change, the laser diodes are assumed to lase at 1.55 μm. And other parameters used in the model are listed in Table 1. The bandwidth of the gain is taken to be about 100 nm and the peak of the gain is positioned at 1.55 μm wavelength.

Table 1 Parameters used in the model

Spontaneous recombination coefficient, B	1×10^{-10} cm^3/s
Auger carrier recombination coefficient, C	1.3×10^{-28} cm^6/s
Transparency carrier density, N_0	1.5×10^{18} cm^{-3}
Effective phase refractive index without injection, $n_{eff,0}$	3.283
Effective group refractive index, n_g	3.7
Thickness of the active layer in the active region, d_{act}	0.048 μm
Thickness of the core in the reflectors, d_{ref}	0.23 μm
Spontaneous coupling factor, β	0.5×10^{-4}
Waveguide loss, α	reflectors 5 cm^{-1} active region 30 cm^{-1}
Linewidth enhancement factor, α_m	3 ~ 8
Nonlinear gain suppression coefficient, ε	10^{-17} cm^3

The power reflectivities for the sampled-grating DBR are calculated using the conventional algorithm and the proposed one. The results are shown in Fig. 2. The conventional algorithm shows the increase of the reflectivity when the refractive index changes, which is impossible as far as no gain or loss change is accompanied. This means that the detuning factor is not correctly incorporated in the conventional algorithm. On the other hand, the new algorithm shows the same peak reflectivity as the refractive index changes, which is physically reasonable.

Fig. 3(a) and 3(b) show the tuning of lasing wavelength and output power of periodically sampled and chirped grating DBR laser diodes due to the change of the refractive index in the rear reflector. The refractive index tuning is assumed to be due to the thermal heating, as shown in Fig. 1.

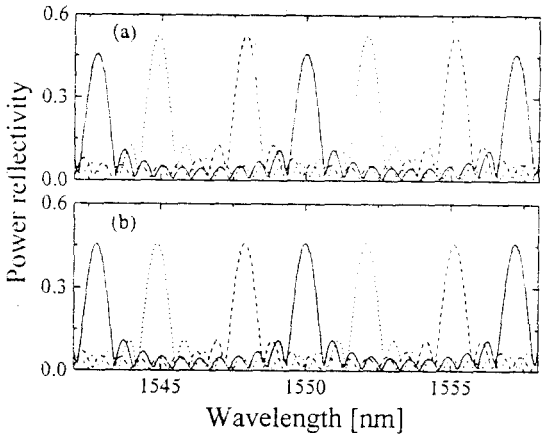

Fig. 2 Comparison of the power reflectivities between (a) the conventional(reference [3]) and (b) the modified algorithm. Wave -guide loss is constant. Dashed line: Δn = -0.005, solid line: Δn = 0.0, dotted line: Δn = 0.005.

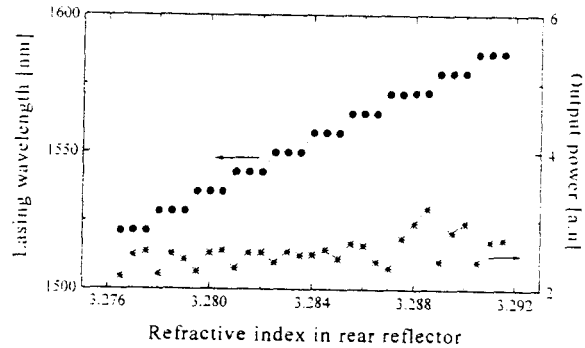

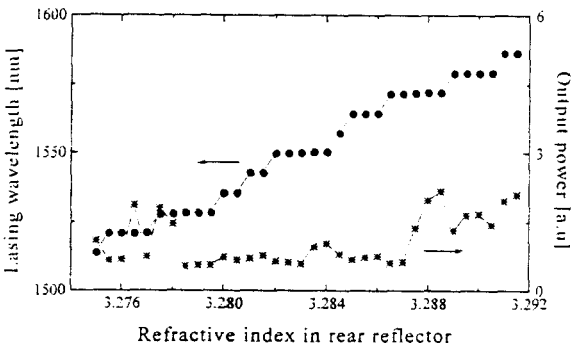

Fig. 3 Tuning property of (a) periodically sampled grating DBR and (b) periodically chirped grating DBR laser diodes.

The tuning range is 64.8 nm and 72 nm with the 7.2 nm interval, respectively, as expected in the separately calculated reflectivity spectrum. Competition between inter-channel modes or intra-channel modes can be observed during the transient state and at some refractive index change. In the vicinity of certain wavelength(for example, 1572 nm), the lasing mode hops by about 52 GHz which is mode spacing of the laser cavity. Lasing mode hopping accompanies the large output power change as shown in Fig. 3. This could be due to the different mirror reflectivities for different longitudinal modes.

The simulation of dynamic responses exhibits the same trend as the measurement[5], as shown in Fig. 4. The bias currents(output powers) are 80 mA(2 mW), 100 mA(2.4 mW), respectively for the sampled and chirped grating DBR laser diodes. The amplitude modulation responses at 200 MHz are 0.053, 0.035 mW/mA, respectively. The AM

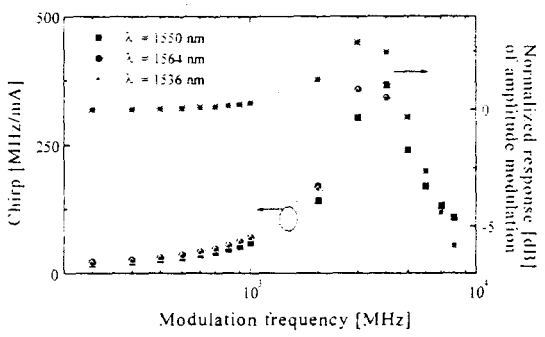

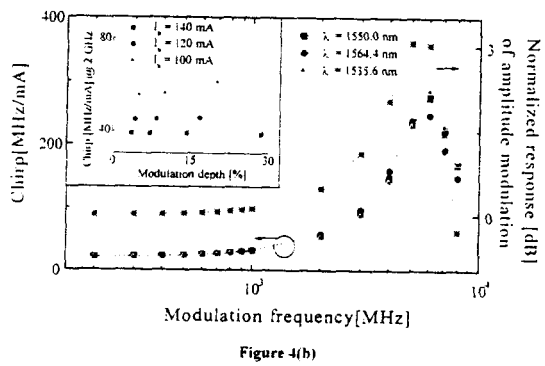

Fig. 4 Dynamic amplitude modulation response and dynamic chirp response of (a) periodically sampled grating DBR and (b) periodically chirped grating DBR laser diodes.

responses at other frequencies are normalized against the value at 200 MHz. For all the stable lasing wavelengths, the chirping is almost the same and increases with the modulation frequency. The chirping properties as a function of modulation depth are also shown in the inset of Fig. 4(b) when the modulation frequency is 2 GHz. The chirping decreases as the bias current(I_b) increases, but it changes little as the modulation depth changes at the fixed bias current. When the modulation depth exceeds the certain range, noticeable harmonic distortion is observed. So only the modulation depths below 30 % are considered in investigating the chirping characteristics. The modulation bandwidth and the relaxation-oscillation frequency, when two mirrors are not biased, are about 5 GHz, 3 GHz, which are very close to the measured values. Dynamic properties of the chirped-grating DBR laser are similar to those of the sampled grating DBR laser, except that the modulation bandwidth and the relaxation-oscillation frequency is higher. This is due to the higher mirror-reflectivity. Linewidth enhancement factor has the relatively large effect on the quantity of the chirping, but has the small effect on the trend shown in Fig. 4. In both cases Fig. 4 (a) and (b), modulation responses of the other lasing wavelength are similar to those of the lasing wavelength when there is no index change in the reflectors. Side-mode rises up when the laser is modulated close to the threshold current. But the quantity is very small and dynamic and static side-mode suppression ratios maintain above 30 dB.

4. The intensity-modulation properties

In this section, the intensity-modulation properties of widely tunable laser diodes integrated with an external EA modulator are investigated. The direct modulation and the external modulation are compared in the aspect of the chirp. And it is shown that the short pulse is generated by driving the external EA modulator sinusoidally.

Figure 5 shows the schematic view of the sampled grating DBR laser diode integrated with an external EA modulator which is driven by the bias voltage and the HF(high frequency) signal. The principle of the intensity modulation is the quantum confined Stark effect in the integrated EA modulator. For the modulator parameters, that is, changes of the absorption coefficients and the refractive index with the bias voltage, the readers are referred to the experimental results of reference [22]. Around the 1.544 μm wavelength, the absorption coefficient(α), and the change of the refractive index(Δn) are given as follows as a 4-th order polynomial function of reverse bias voltage(V): $\alpha\ [cm^{-1}] = 3.3412\times V^4 - 60.3236\times V^3 + 282.1953\times V^2 + 192.9116\times V + 745.0217$, and $\Delta n = -0.0001\times V^4 + 0.0013\times V^3 - 0.0089\times V^2 + 0.0213\times V + 0.0007$. The absorption coefficient and the refractive index change as a function of V at other wavelengths such as λ = 1557.2 nm and λ = 1535.6 nm can be interpolated from the experimental data presented in reference [22].

The lasing section is switched on from just below the threshold to well above. During this period, the modulator is kept at 4 V bias to give significant absorption. After the lasing section, which is composed of the active region and periodically sampled-grating DBR, is stabilized, the voltage applied to the modulator is modulated at the rate of 5 Gbps from 4 V to 0 V. A simplified parasitic network with time constant $(RC)^{-1}$ = 25 ps is used in the analysis in order to simulate more realistic modulation than simply modulating with a square wave. And both facets of the device are assumed to be anti-reflection coated.

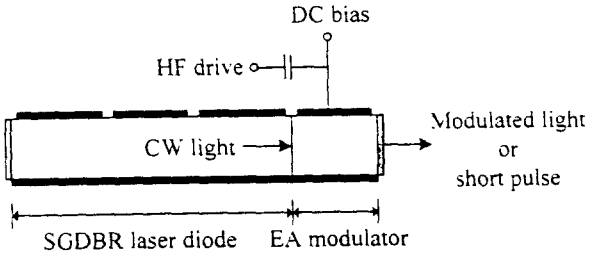

Fig. 5 Schematic view of a SGDBR (sampled grating distributed Bragg reflector) laser diode integrated with an external EA(electro - absorption) modulator.

Figure 6 shows the optical power from the modulator and its chirp during the intensity-modulation. It is shown that output power is modulated at 5 Gbps and swings from 0 to 3.5 mW giving the extinction ratio of about 23 dB. As

indicated in the Figure 6(a), as the modulator switches on and off, the optical output when the power reflectivity of the modulator facet is 0.0 % changes with the rising time corresponding to the time constant, while the optical output when the power reflectivity of the modulator facet is 0.1 % has the slight fluctuation, which is due to the fact that the feedback light reflected at the modulator facet has the effect on the lasing of the active region. In the Figure 6(b), the chirp of the optical output power is evaluated from the instantaneous frequency ω(t) given by

$$\omega(t) = \frac{d\phi_{out}}{dt} = \mathrm{Im}\{\ln(E_{out})\} \qquad (10)$$

where E_{out} and ϕ_{out} are the optical complex field and its phase output from the modulator. Im{ } stands for the imaginary part. In general, ω(t) calculated from (10) is noisy because of the spontaneous emission noise in the active region. But, after the lasing section is stabilized, the stimulated emission becomes dominant, so that noise-free ω(t) can be obtained easily by neglecting the spontaneous emission in the analysis. The spike shown in the chirp is resulted from the refractive index change in the EA modulator. As Δn(t) is the function of reverse bias voltage, indicated in the above, the on/off modulation of the reverse bias voltage causes the steep change of the refractive index at the time of switching. The asymmetry of the spike is due to the nonlinearity of the refractive index with the voltage. Although the peak-to-peak of the spike goes up to 15 GHz, it exists for a little time less than a tenth of the pulse width of 200 ps, and consequently contributes little energy to the overall average chirp. As shown in the figure 6(b), there is no frequency difference between the "on" and "off" state when the power reflectivity of the modulator is 0.0 %, while there is a frequency difference of several hundreds of MHz between the "on" and "off" state when the power reflectivity of the modulator is 0.1 %. This is due to the feedback light at modulator facet, which also causes the fluctuation in the optical power, shown in the figure 6(a). The phase of the power reflectivity is 0°.

Figure 7 shows the comparison of the frequency chirps between the external modulation

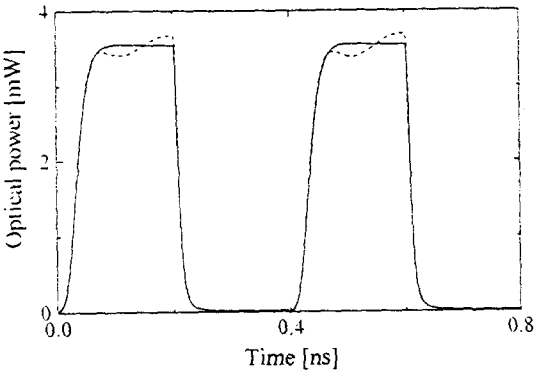

Figure 6(a)

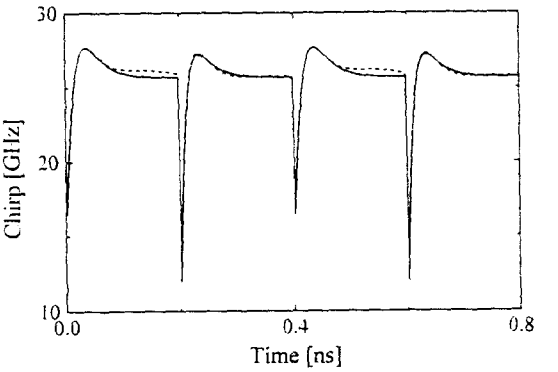

Figure 6(b)

Fig. 6 Intensity-modulation properties of a SGDBR laser diode integrated with an EA modulator. An EA modulator is driven from 4 V to 0 V by a reverse bias voltage and a HF drive whose frequency is 5 Gbps. (a) the optical power output and (b) its instantaneous frequency chirp. Solid line: R_{mod} = 0.0 %, dashed line: R_{mod} = 0.1 %, where R_{mod} is the power reflectivity of the modulator facet.

and the direct modulation of the laser diode. The frequency chirp in this paper is defined to be $\Delta f_{on} - \Delta f_{off}$, where $\Delta f_{on,off}$ are the frequency chirps for the "on" and "off" states when the output powers are in steady-state, respectively. The frequency chirp of the external modulation is calculated by the same method that is used in the analysis of the figure 6. The power reflectivity of the modulator facet is 0.1 %. In the direct modulation, after the optical power is stabilized, the injection current into the active region is modulated at 5 Gbps to make the extinction ratio 20 dB. The frequency

chirp of the external modulation varies from -0.7 to 0.4 GHz, while that of the direct modulation is from -9.2 to 12.6 GHz, for the phases of the modulator facet from 0° to 360°.

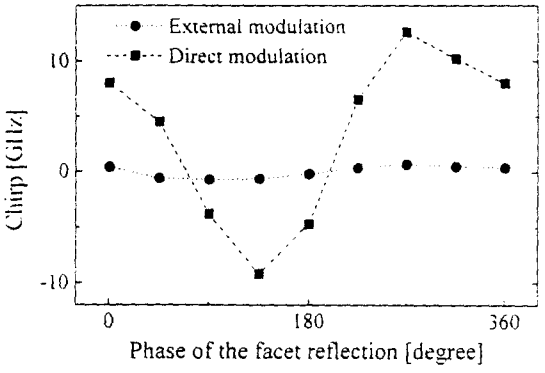

Fig. 7 Comparison of the frequency chirp for the phase of the facet reflection between an external modulation and a direct modulation. The extinction rations are about 23 dB, 20 dB, respectively.

Figure 8 shows the wavelength dependence of the frequency chirp. The SGDBR laser diode is tuned to be lasing at 1557.2 nm, 1542.8 nm, and 1535.6 nm, respectively, and the external electroabsorptive modulator is modulated at the rate of 5 Gbps from 4 V to 0 V. It is shown that the frequency chirps decrease as the injection current into the gain section increases. For a 1557.2 nm wavelength, the frequency chirp shows the negative value at injection currents greater than 110 mA, which is due to the strong feedback light reflected at the modulator facet. In this case, the feedback light is relatively stronger because the modulator has the smaller change of the absorption around the 1557.2 nm wavelength, and at this wavelength the refractive index increase in the modulator for the "on" state is smaller than that for the "off" state, as indicated in reference [22]. And, for all the wavelengths considered in the figure 8, the frequency chirps do not exceed 0.3 GHz, which is much lower than that of the direct modulation.

sinusoidal modulation of the external electroabsorptive modulator integrated into the continuous wave laser diode. Figure 9 shows a pulse compared with the soliton and the pulse train,

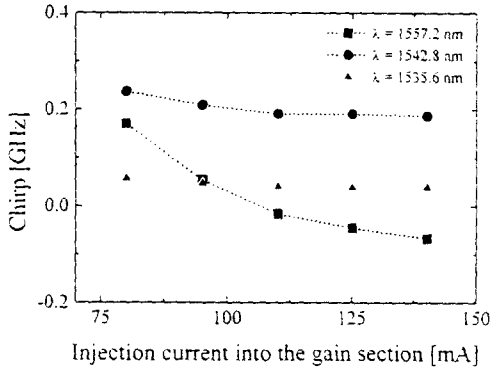

Fig. 8 The wavelength dependence of the frequency chirp. The external modulator is modulated at the rate of 5 Gbps from 4 V to 0 V, and the power reflectivity and its phase of the modulator facet is 0.1 % and 0°.

which are emitted from the external modulator. The applied reverse voltage to the modulator varies from 0 to 8 V sinusoidally and its frequency is 30 GHz. Continuous lightwave from the lasing section is gated optically by the absorption of the external modulator which is modulated by the applied voltage. As shown in the figure 9, the generated pulse is curve-fitted well to the $\mathrm{sech}^2(\tau)$ which is the waveform of the soliton. The pulse repetition rate 30 Gbps, and the $\Delta\tau$ and $\Delta\nu$ of the generated pulse are about 2.294 ps, and 182 GHz,

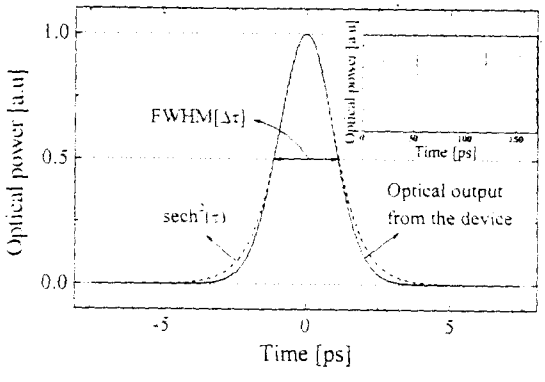

Fig. 9 The generated short pulse train and its comparison with the soliton. The pulse repetition rate is 30 Gbps corresponding to the modulation frequency. Time FWHM, $\Delta\tau$ = 2.294 ps, frequency FWHM, $\Delta\nu$ = 182 GHz and time-bandwidth product, $\Delta\tau\,\Delta\nu$ is 0.418.

respectively. The time-bandwidth product is 0.418, which means that the generated pulse is nearly transform-limited.

5. Conclusion

An improved time-domain large signal model is developed for analyzing the widely tunable laser diodes integrated with periodically sampled- and chirped-grating DBR and an external EA modulator. The model is demonstrated to be very useful in simulating the wide tuning due to the refractive index change of the passive section of the complex laser diodes. First, using an improved time-domain model, the dynamic tuning characteristics of the laser diodes incorporating the sampled-grating DBR and chirped-grating DBR are investigated, respectively. Second, the intensity-modulation properties of the sampled-grating DBR laser diode integrated with an EA modulator are discussed. It is shown that the frequency chirps of the external modulation at several lasing wavelengths are below 0.3 GHz, which indicates the low chirp operation over the wide tuning range. And also the transform-limited pulse train is generated by the optical gating of the EA modulator, from which it is expected that the widely tunable soliton can be generated by the laser diodes integrated with periodically sampled- and chirped-grating DBR and an EA modulator.

References

1. M. S. Borella, J. P. Jue, D. Banerjee, B. Ramamurthy, and B. Mukherjee, "Optical components for WDM lightwave networks," Proc. IEEE, vol. 85, no. 8, pp. 1274-1307, 1997.
2. P. E. Green, *Fiber Optic Networks*, Prentice Hall, Englewood Cliffs, NJ, 1993.
3. J. F. L. Devaney, W. Forysiak, N. J. Smith, and N. J. Doran, "WDM of enhanced power solitons in strongly dispersion-managed systems," in Optical Fiber Commun. Conf., Opt. Soc. Amer., Dallas, 1997, ThN3, pp. 306-307.
4. V. Jayaraman, Z. M. Chuang, and L. A. Coldren, "Theory, design, and performance of extended tuning range semiconductor lasers with sampled gratings," IEEE J. Quantum Electron., vol. 29, no. 6, pp. 1824 - 1834, 1993.
5. S. L. Lee, D. A. Tauber, V. Jayaraman, M. E. Heimbuch, L. A. Coldren, and J. E. Bowers, "Dynamic responses of widely tunable sampled grating DBR lasers," IEEE Photon. Technol. Lett., vol. 8, no. 12, pp. 1597 - 1599, 1996.
6. C. K. Gardiner, R. G. S. Plumb, P. J. Williams, and T. J. Reid, "Three-section sampled-grating DBR lasers: modelling and measurements," IEE Proc.-Optoelectron., vol. 143, no. 1, pp. 24 - 30, 1996.
7. F. Kano, H. Ishii, Y. Tohmori, and Y. Yoshikuni, "Characteristics of super structure grating(SSG) DBR lasers under broad range wavelength tuning," IEEE Photon. Technol. Lett., vol. 5, no. 6, pp. 611 - 613, 1993.
8. H. Ishii, H. Tanobe, F. Kano, Y. Tohmori, Y. Kondo, and Y. Yoshikuni, "Quasicontinuous wavelength tuning in super-structure-grating(SSG) DBR lasers," IEEE J. Quantum Electron., vol. 32, no. 3, pp. 433 - 441, 1996.
9. B. S. Kim, J. K. Kim, Y. Chung, and S. H. Kim, "Time-domain large signal analysis of widely tunable DBR laser diodes with periodically sampled and chirped gratings," IEEE Photon. Technol. Lett., vol. 10, no. 1, pp. 39 - 41, 1998.
10. B. S. Kim, Y. Chung, and S. H. Kim, "A study on the characteristics of a widely tunable sampled grating DBR laser diode integrated with an external modulator," J. of Korea Electronics Engineers-A, vol. 33, pp. 174 - 185, 1996.
11. K. Wakita, K. Sato, I. Kotaka, M. Yamamoto, and M. Asobe, "Transform-limited 7-ps optical pulse generation using a sinusoidally driven InGaAsP/InGaAsP strained multiple-quantum-well DFB laser/modulator monolithically integrated light source," IEEE Photon. Technol. Lett., vol. 5, pp. 899 - 901,

This paper was also published on IEICE Transactions on Electronics, Vol. E81-C, No. 8, August 1998.